The Neutral ISM in Starburst Galaxies
*ASP Conference Series, Vol. **VOLUME**, 2003*
Susanne Aalto & Susanne Huttemeister, eds

IR emission from AGNs

Moshe Elitzur
Department of Physics and Astronomy, University of Kentucky, Lexington, KY 40506, USA

Maia Nenkova
Department of Physics and Astronomy, University of Kentucky, Lexington, KY 40506, USA

Željko Ivezić
Astrophysical Sciences Department, Princeton University, Princeton, NJ 08544, USA

Abstract. Unified schemes of active galactic nuclei (AGN) require an obscuring dusty torus around the central source, giving rise to type 1 line spectrum for pole-on viewing and type 2 characteristics in edge-on sources. Infrared radiation at its different wavelengths is the best probe of the dust distribution, whether the torus orientation is edge-on or pole-on. The observed IR is in broad agreement with the unified scheme but serious problems remained in all early modeling efforts. In spite of a general awareness that the dust must be concentrated in clouds, clumpiness remained the one major ingredient missing in those radiative transfer studies because of the inherent difficulties it presents. We have recently developed the formalism to handle dust clumpiness and our results indicate that its inclusion may resolve the difficulties encountered by the previous theoretical efforts. We show that these problems find a natural explanation if the dust is contained in $\sim$ 5–10 clouds along radial rays through the torus. The spectral energy distributions (SED) of both type 1 and type 2 sources are properly reproduced from different viewpoints of the same object if the optical depth of each cloud is $\gtrsim 40$ at visual wavelengths and the clouds' mean free path increases roughly in proportion to radial distance.

1. Introduction

Although there is a bewildering array of AGN classes, a unified scheme has been emerging steadily (e.g. Antonucci 1993, 2002; Wills 1999). The nuclear activity is powered by a supermassive ($\sim 10^6$–10^9 $M_\odot$) black hole and its accretion disk, which extends to $\sim$ 1 pc. This central engine is surrounded by a dusty toroidal structure, extending to $\gtrsim$ 100 pc. Much of the observed diversity is simply the result of viewing this axisymmetric geometry from different angles.

The torus provides anisotropic obscuration of the central region so that sources viewed face-on are recognized as Seyfert 1 galaxies, those observed edge-on are Seyfert 2. The primary evidence for the torus comes from spectropolarimetric observations of type 2 sources, which reveal hidden type 1 emission via reflection off material situated above the torus opening. While compelling, this evidence is only indirect in that it involves obscuration, not direct emission by the torus itself.

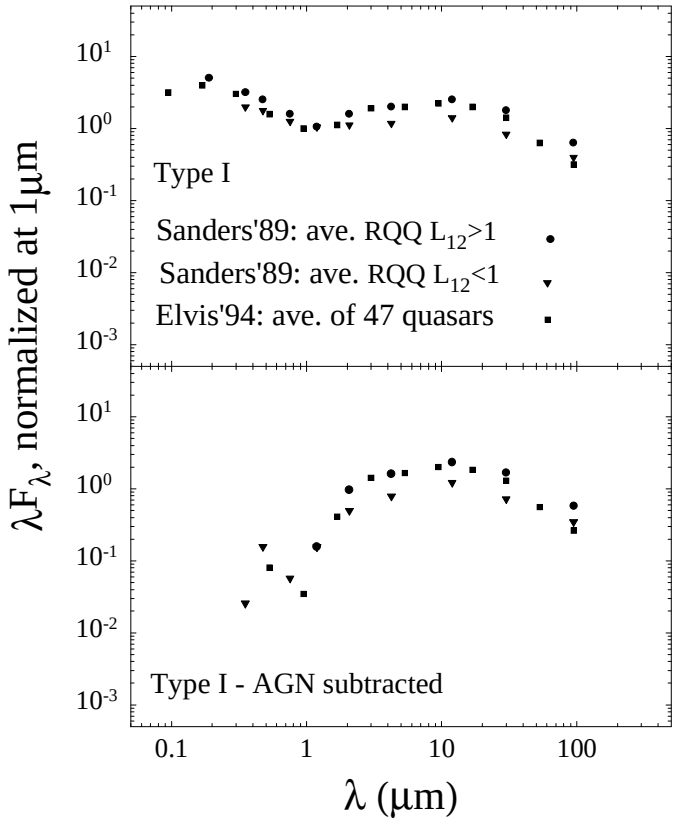

Figure 1. SED's of type 1 sources. Top: Average spectra from the indicated compilations. Bottom: The same SED's after subtracting a power law fit through the short wavelengths ($\lesssim 1\mu$m). These AGN-subtracted SED's are similar to those of typical type 2 sources.

An obscuring dusty torus should reradiate in the IR the fraction of nuclear luminosity it absorbs, and the continua from most AGN indeed show significant IR emission. The top panel of figure 1 shows composite SED's of type-1 sources from compilations by Sanders et al (1989) and Elvis et al (1994). The power law emission at short wavelengths is the expected behavior from the AGN accretion disk and the excess at $\lambda \gtrsim 1\mu$m is attributed to radiation reprocessed by the dusty torus. Subtraction of the power law produces the SED's shown in the bottom panel, which are indeed very similar to those of typical type-2 sources, in accordance with unified schemes.

Pier & Krolik (1992, 1993) were the first to explore the effects of toroidal geometry on dust radiative transfer. They noted that the AGN dust must be concentrated in clouds to protect the grains, but because of the difficulties in modeling a clumpy medium approximated the density distribution with a uniform one instead. Still, the directional dependence of their model radiation did reproduce the gross features of observed SEDs, indicating that the toroidal geometry captures the essence of IR observations. But major problems remained:

1. The models could not generate sufficient emission over the full range of observed far-IR wavelengths.

2. The extreme column densities ($\gtrsim 10^{25}$ cm^{-2}) found in subsequent x-ray observations greatly exceeded the values allowed by the models. In particular, such large columns imply extremely deep 10μm absorption feature in type 2 sources, contrary to observations which reveal only moderate depths.

3. Type 1 sources do not show any evidence of the 10μm silicate feature, neither in emission nor absorption (e.g., Spoon et al 2003). Such behavior is reproduced only in a narrow, finely-tuned range of the model parameters.

4. The huge variation of torus obscuration corresponding to the range of columns densities found in type 2 x-ray observations (10^{21}–10^{25} cm^{-2}) implies large variation among SEDs, incommensurate with the rather modest variation displayed by the observations.

These problems persisted in all the following studies, which also employed continuous density distributions (e.g., Granato & Danese 1994; Efstathiou & Rowan-Robinson 1995). Rowan-Robinson (1995) noted that a more realistic model of the torus would place the dust in clouds and suggested that clumpiness might alleviate these problems, but was unable to offer a proper treatment of clumps.

2. Emission from a clumpy medium

A fundamental difference between clumpy and continuous density distributions is that radiation can propagate freely between different regions of an optically thick medium when it is clumpy, but not otherwise. We have recently developed a detailed formalism for emission from a clumpy medium and applied it to the AGN obscuring torus (Nenkova, Ivezić & Elitzur 2002, NIE hereafter, and in preparation). The building block of our formalism is a single cloud heated both directly by the AGN and by all other clouds. The direct heating introduces dependence on the position-angle around the AGN since the dust temperature is much higher on the cloud's illuminated face than on any other part of its surface. Therefore the radiation from the cloud depends both on its distance from the AGN (which controls the highest temperature in the cloud) and the position angle between the AGN, cloud and observer. We have devised a method for realistic construction of "synthetic clump" source function $S_{c\lambda}$ that accounts for this effect and employs an exact solution of radiative transfer including scattering, absorption and emission by optically thick dust. The solution is performed

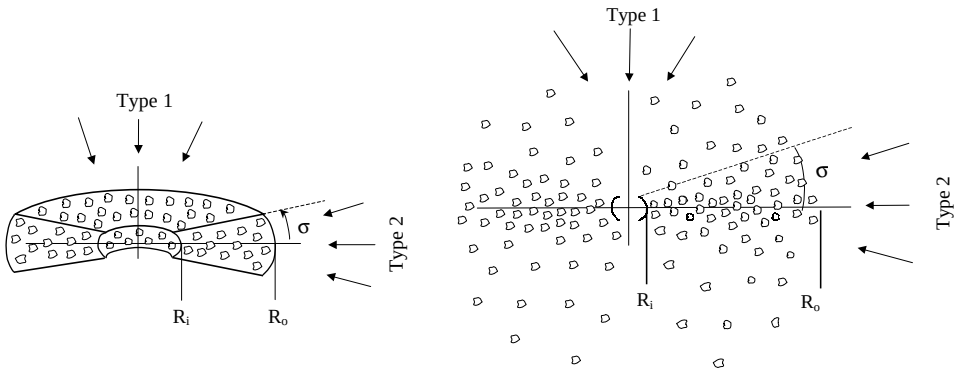

Figure 2. Geometry for modeling AGN clumpy tori between radii $R_{\rm i}$ and $R_{\rm o}$. The angular distributions are characterized by a width parameter σ. The step-function distribution on the left has a sharp boundary, the one on the right is smeared, e.g. Gaussian.

with the code DUSTY (Ivezić, Nenkova & Elitzur 1999). The absorption and scattering coefficients are those of standard interstellar dust.

Given these building blocks, we have developed an exact formalism for the emission when all the dust is in clouds and the cloud distribution follows Poisson statistics. For simplicity, each cloud has the same optical depth τ_λ, radius R_c and volume $V_c \simeq A_c R_c$ where A_c is the cloud area. The mean number of clouds encountered in segment ds along a given path is $d\mathcal{N}(s) = ds/\ell(s)$, where $\ell = (n_c A_c)^{-1}$ is the mean free path between clouds (n_c is the number density of clouds). The volume filling factor of the cloud population is then

$$\phi = n_c V_c = \frac{R_c}{\ell} \tag{1}$$

We adopt as the definition of clumpiness the condition $R_c \ll \ell$, i.e., $\phi \ll 1$, small volume filling factor. Under these circumstances, each cloud can be considered a point source of intensity $S_{c\lambda}$, and the intensity generated along the segment is $S_{c\lambda} d\mathcal{N}$. Denote by $P_{\rm esc}$ the probability that this radiation propagate along the rest of the path without absorption by any other cloud. Natta & Panagia (1984) show that Poisson statistics for the clump distribution yields

$$P_{\rm esc} = e^{-t_\lambda}, \qquad \text{where} \quad t_\lambda = \mathcal{N}(s)(1 - e^{-\tau_\lambda}) \tag{2}$$

and $\mathcal{N}(s) = \int_s d\mathcal{N}$ is the mean number of clouds along the rest of the path. The intuitive meaning of this result is straightforward in limit cases. When $\tau_\lambda < 1$ we simply have $P_{\rm esc} = e^{-\tau_{\rm tot}}$, the probability to escape from a continuous medium with overall optical depth $\tau_{\rm tot} = \mathcal{N}\tau_\lambda$. That is, the clumpiness becomes irrelevant. It is important to note that $\tau_{\rm tot}$ can be large, the only requirement for this limit is that each cloud be optically thin. The opposite limit $\tau_\lambda \gg 1$ gives $P_{\rm esc} = \exp(-\mathcal{N})$. Even though each clump is optically thick, a photon can still escape if it avoids all the clumps along the path.

With this result, the contribution of segment ds to the emerging intensity is simply $P_{\rm esc}S_{c\lambda}d\mathcal{N}$ and the overall intensity of a clumpy medium is thus

$$I_\lambda^{\rm C} = \int e^{-t_\lambda} S_{c\lambda}(s) d\mathcal{N}(s), \tag{3}$$

which bears great resemblance to the formal solution of the radiative transfer equation for continuous medium. This result is rather straightforward and can be easily generalized to handle configurations in which the clumps have different properties, and even extended to line radiation. The flux at distance D is simply $F_\lambda^{\rm C} = \int I_\lambda^{\rm C} dA/D^2$ where dA is the surface area element perpendicular to the line of sight.

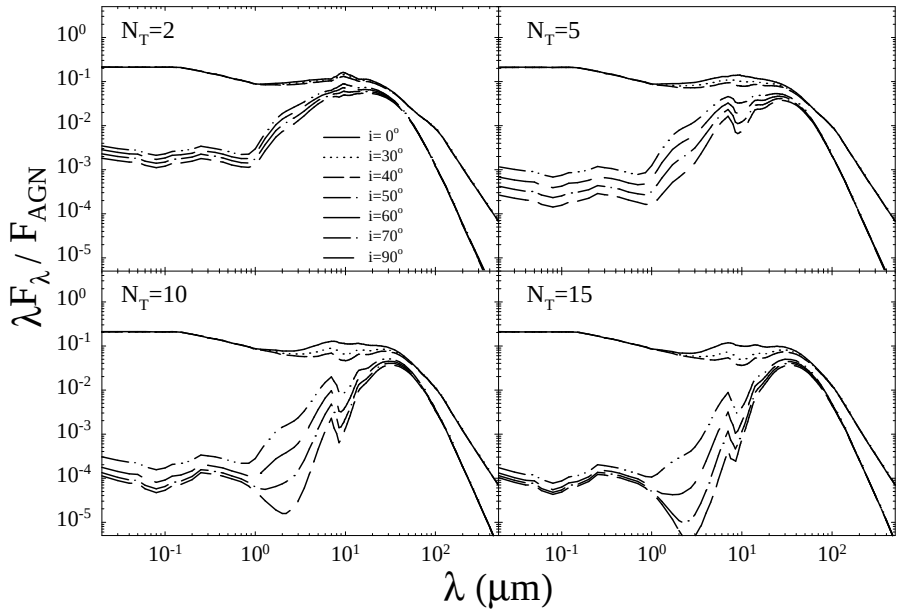

Figure 3. Sample model SEDs. The number of clouds $\mathcal{N}_{\rm T}$ and the viewing angle from the torus axis are indicated. In all models, each cloud has optical depth $\tau_{\rm V} = 60$, the cloud radial distribution extends to $R_{\rm o} = 100R_{\rm i}$ with the mean free path increasing in proportion to r. The angular distribution is Gaussian with $\sigma = 45°$. (Nenkova, Ivezić & Elitzur, in preparation).

3. Application to AGN

After constructing the clump data base, we applied the formalism to AGN emission by integrating over toroidal distributions of dusty clouds extending from inner radius $R_{\rm i}$ to $R_{\rm o}$, as shown in figure 2. In all calculations $R_{\rm i}$ occurs where the dust temperature reaches 1400 K, the temperature above which all grains evaporate. This choice implies $R_{\rm i} = 1.02\, L_{12}^{1/2}$ pc for an AGN luminosity $L_{12} = L/10^{12}L_\odot$. The cloud radial distribution is described by $\mathcal{N}_{\rm T}$, the mean

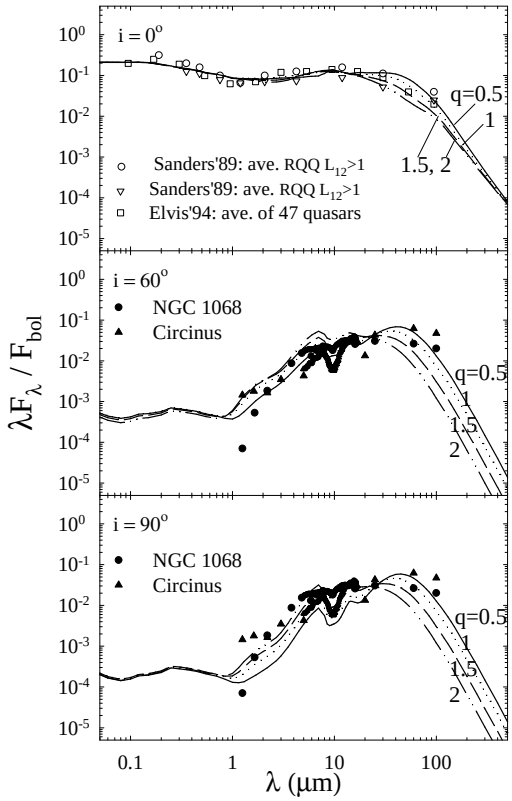

Figure 4. Model results for the indicated viewing i from the axis of a sharp-edge torus with $\sigma = 45°$, $R_o = 100R_i$ and $\mathcal{N}_T = 5$ clouds with $\tau_V = 60$ each. The clouds' mean free path varies as r^q, with the indicated q. The top panel data are type 1 composite spectra. Data in the bottom panels are for the Seyfert 2 NGC 1068 and Circinus.

number of clouds along a ray through the torus equator, and the index q of the power law r^q we employ for the radial variation of the mean free path between clouds. The angular distribution is specified by a width parameter σ. In NIE we report results for sharp-edge step function angular distributions. We have since explored continuous distributions and found that Gaussian generally produces better agreement with observations. The final input is τ_V, the optical depth of each cloud at visual wavelengths.

Figure 3 shows some sample SED's for a set of typical parameters. Models with only 2 clouds along equatorial rays display a trace of the 10μm feature in emission and thus cannot correspond to the bulk of observed sources. Similarly, at $\mathcal{N}_T = 15$ the near- and mid-IR emission is suppressed too much. Models with $\mathcal{N}_T = 5$–10 clouds produce SED's that closely resemble observations. It is noteworthy that none of the models displays any of the severe problems that afflicted those with continuous dust distributions.

According to unified schemes, viewing the same torus from the directions shown in figure 2 should give rise to the SEDs observed in type 1 and type

2 sources. Figure 4 shows sample model outputs and data. Each data set was scaled for a rough match of the model results without attempting a best fit. The scaling factor determines the bolometric flux $F_{\rm bol}$, a quantity inaccessible for direct measurement for type 2 objects. The panels for $i = 0°$ and $90°$ reproduce results presented in NIE, the $i = 60°$ panel is a recent result from work in progress. Data points for type 1 sources show the average spectra for radio-quiet quasars and Seyfert 1 galaxies, displayed already in figure 1. Because of the high obscuration of the AGN in type 2 sources, fluxes for their nuclear regions properly extracted out of the contributions of the host galaxy and starburst regions are scarce. The data shown are for the prototype Seyfert 2 NGC 1068 and Circinus. As is evident from the figure, it is possible to reproduce the IR emission from both type 1 and type 2 sources at different viewing angles of the same clumpy torus, in accordance with unified schemes. It is interesting that the "generic" type 2 inclination angle $i = 90°$ fails to produce the near IR emission from NGC 1068 and Circinus, but the problem is solved by our new results for $i = 60°$. Indeed, Bock et al (2000) conclude from Keck imaging observations that the inclination is $\sim 65°$.

The intrinsic luminosity is unobservable in type 2 sources because the bulk of the radiation is emitted along directions close to the torus axis. This persistent problem has especially serious implications for the cosmic x-ray background (Mushotzky et al 2000). X-ray observations have demonstrated that there is a large population of heavily obscured AGN, but are unable to measure the absorbed power with any precision; only IR observations can accomplish this task. Attempts to determine empirical correlations between the intrinsic x-ray and mid-IR emission have been made in various observational studies (e.g., Alonso-Herrero et al 2001, Krabbe et al 2001). Detailed fits to the SED of individual sources offer a new, reliable handle on the intrinsic luminosity — the overall scaling factor that matches the observed flux density to the best-fit model SED is simply the AGN bolometric flux $F_{\rm bol}$.

From comparison with overall properties of observed SED's, and especially the CfA sample of Seyfert galaxies (Alonso-Herrero et al 2003), we find that the following set of parameters describes adequately the data:

- Gaussian angular distribution with $\sigma = 45° \pm 15°$
- Average number of clouds along equatorial radial rays $\mathcal{N}_{\rm T} = 5$–10
- $q = 1$–2 for the r^q behavior of the mean free path between clouds
- Torus outer radius $R_{\rm o}$= (10pc – 100pc)$\times L_{12}^{1/2}$
- Cloud optical depth at visual $\tau_{\rm V} \geq 40$

The last two points deserve further discussion.

3.1. Torus dimensions

The listed range of acceptable $R_{\rm o}$ ensures proper reproduction of observed SEDs. However, pinning down the actual torus size within this range is surprisingly difficult even with high-resolution imaging observations. Figure 5 shows the intensity profiles at various wavelengths for a torus with $R_{\rm o} = 100R_{\rm i}$. One

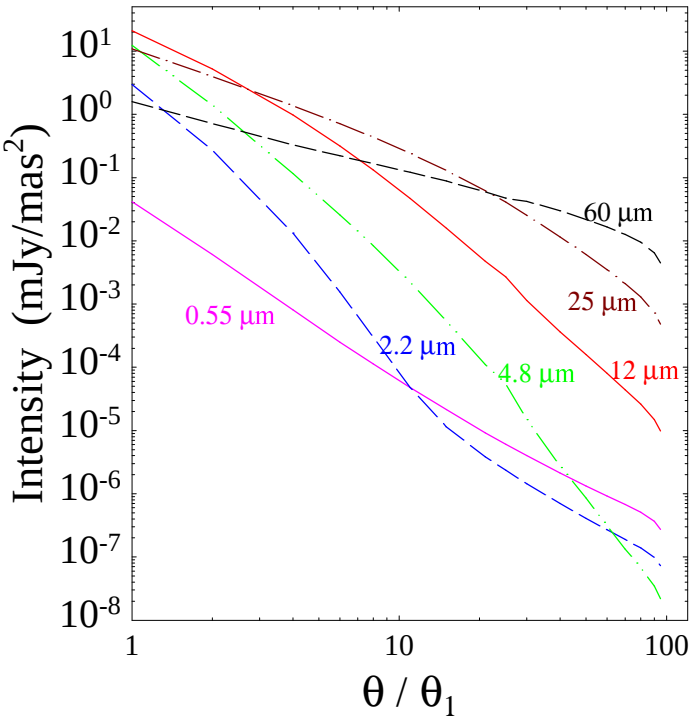

Figure 5. Model predictions for intensity profiles at various wavelengths for a face-on torus with a Gaussian angular distribution of clouds and $R_{\rm o} = 100\,{\rm pc}\times L_{12}^{1/2}$. The angular scale θ_1 is $0\farcs02$ for a source with $L_{12} = 1$ at a distance of 10 Mpc.

striking aspect is the rapid decline of brightness with distance from the AGN. The torus is the brightest at 12μm but even at this wavelength the FWHM is only $\sim 2\theta_1$, and the angular scale θ_1 is a mere $0\farcs02$ for a $10^{12}L_\odot$ source at a distance of 10 Mpc. The small dimensions imply that current facilities cannot resolve the torus even in the most nearby sources. In particular, the $\sim 0\farcs3$ structure visible at the core of NGC 1068 in mid-IR Keck imaging by Bock et al (2000) reflects instrumental resolution, not the actual torus size. The torus inner region will be resolvable by the VLTI at its promised angular resolution of milli-arcsecond at the J-band.

Another problem is that a small torus appears practically indistinguishable from the inner regions of a larger one. For example, the $\theta \le 30\theta_1$ portions of the plots in figure 5 are virtually identical to the full brightness profiles of a torus with $R_{\rm o} = 30R_{\rm i}$. Because the near and mid-IR brightness decline by more than two orders of magnitude already within $10\theta_1$, the torus outer regions will remain hidden whenever viewed with instruments with dynamical range of 10^2–10^3, and its size will be underestimated. Thanks to a more moderate brightness decline, longer wavelengths are more suitable for actual measurements of the torus true size. Only imaging at $\sim 60\mu$m by ALMA holds the promise of distinguishing a 30pc torus from a 100pc one in the foreseeable future.

3.2. Cloud optical depths

Significantly, the only constraint on the optical depth of individual clouds is the lower bound $\tau_V \gtrsim 40$. The model results vary only slightly when τ_V increases from 40 to 100, and hardly at all during further increase. The reason is simple. The dependence on τ_V arises from the probability for photon escape and the cloud source function, and both factors approach saturation at large τ_V. From eq. 2, $P_{esc} = e^{-\mathcal{N}}$ whenever $\tau_\lambda \gg 1$, and at $\tau_V \gtrsim 40$ this condition is met at all relevant wavelengths. Similarly, because each cloud is heated from outside, only its surface is heated significantly when τ_V is large. Increasing τ_V further only adds cool material, thus $S_{c\lambda}$ saturates for all relevant λ (similar to standard black-body emission). Extending our calculations all the way to $\tau_V = 500$, we have verified that increasing τ_V indeed has no effect on the model results.

This explains at once the surprisingly small variation among AGN SED's in spite of the huge range of torus columns. From x-ray measurements of 73 Seyfert 2 galaxies Bassani et al (1999) find a large variation in column density, with a mean of $3{\times}10^{23}$ cm^{-2} and $\gtrsim 10^{24}$ cm^{-2} for as many as a third of the sources. This mean is comparable with the column density of our torus for standard dust-to-gas ratio and 5 clouds of $\tau_V \gtrsim 40$ each. Furthermore, a natural consequence of our model is the observed similarity of SED among type 2 sources in spite of the large x-ray column variation: since τ_V is bounded only from below, the SED remains the same at all $\lambda \gtrsim 1\mu$m for arbitrary increase in overall column. In contrast, the x-ray absorption does vary with τ_V because the optical depth for Thomson scattering is only $\sim 10^{-2}\tau_V$ so that each cloud remains mostly optically thin. Sources with small columns may show up in x-ray absorption while selectively excluded from IR observations because of their weak emission.

4. Torus Mass

Risaliti, Maiolino & Salvati (1999) note that the large column densities discovered in x-ray absorption imply torus masses in excess of the dynamical mass, posing a problem for the system stability. For a continuous mass distribution ($\phi = 1$), the relation between the torus mass M_{torus} and the hydrogen overall column density $N_{H,tot}$ can be written as

$$\phi = 1: \qquad M_{torus} = m_H N_{H,tot} \Omega < r^2 >_{gas} \tag{4}$$

Here m_H is the H-mass, Ω is the solid angle subtended by the torus at the AGN and $< r^2 >_{gas}$ stands for the average of r^2 weighted with the gas density distribution. The corresponding relation for a clumpy torus is

$$\phi \ll 1: \qquad M_{torus} = m_H \mathcal{N}_T N_{H,C} \Omega < r^2 >_{clouds} \tag{5}$$

Here $N_{H,C}$ is the column density of a single cloud and $< r^2 >_{clouds}$ stands for the average of r^2 weighted with the cloud number distribution. Surprisingly, perhaps, the relation for a clumpy torus does not involve the volume filling factor. Apart from the different average weighting functions, the two relations give identical masses for the same overall columns $N_{H,tot} = \mathcal{N}_T N_{H,C}$. However, continuous distribution usually must be flat to place enough material at large

distances and produce the long wavelength emission. Cloud distributions are steeper in comparison, because the AGN radiation can reach further thanks to the clumpiness, resulting in smaller $< r^2 >$. With typical parameters, the torus mass ranges from 10^5–10^7 $M_\odot$, alleviating the mass problem.

5. Probes of Cloud Distribution

Our results add strong support for AGN unification schemes. In accordance with such schemes, the IR emission from both type 1 and type 2 sources is reproduced at different viewing of the same geometry. Our analysis establishes for the first time the constraints imposed by the IR emission on cloud distributions, not just overall column densities. The distribution is described by q and $\mathcal{N}_{\rm T}$, individual clouds by their optical depth $\tau_{\rm V}$. No other cloud property was specified. The cloud size enters only indirectly through the underlying assumption $R_c \ll \ell$, i.e., $\phi \ll 1$. A reasonable realization, though not unique, of this assumption is a constant $\phi = 0.1$ throughout the torus. For a model with $q = 1$, $\mathcal{N}_{\rm T} = 5$, $\tau_{\rm V} = 100$ and $L_{12} = 1$ this implies clouds that vary from $R_c \sim 0.1$ pc with gas density $\sim 3{\times}10^5$ cm^{-3} in the torus inner regions to $R_c \sim 10$ pc with density $\sim 3{\times}10^3$ cm^{-3} at the outer edge, resembling ordinary molecular clouds.

The IR flux involves integration over the full volume, summing up the contributions of many lines of sight. By contrast, x-ray absorption measures the properties of the cloud distribution along a single line of sight. A recent study by Risaliti, Elvis & Nicastro (2002) finds x-ray variability on all available time scales—from months to 20 years, with the latter simply marking the longest time span currently in the data archives. They conclude that the x-rays are absorbed by clouds belonging to two populations. The first one includes clouds at very short distances ($\lesssim 10^{17}$ cm) from the AGN. These are dust free as they are located within the dust sublimation radius. The second involves clouds at $\sim$ 5–10 pc, presumably in the dusty torus. The scenario Risaliti et al propose is similar to a disk-driven hydromagnetic wind which uplifts, by its ram pressure, and confines, by its magnetic pressure, dense clouds fragmented from the disk. In the wind inner regions the clouds are dust free, beyond the sublimation distance they become dusty (Kartje, Königl & Elitzur 1999).

Type 1 are distinguished from type 2 sources by the visible AGN contribution they display. In a clumpy torus, especially with Gaussian edges, the distinction between the two classes becomes an issue of probability. In spite of the strong variation with viewing angle, there is always a finite probability for an unperturbed line of sight to the AGN even in the torus equatorial plane. Such a source would be classified as type 1 in contrast with the strict interpretation of unified schemes. The few recorded transitions between type 1 and 2 may correspond to transits of obscuring clouds across the line of sight to the AGN.

Our formalism currently handles only the simplest case where all clouds have identical properties and no intercloud medium. Additional clouds with smaller $\tau_{\rm V}$ would make little contribution to IR emission but could absorb the radiation from the dominant clouds, thus significantly affecting the overall SED. The same goes for intercloud medium with $\tau_{\rm V} \sim$1–5. We plan to expand our formalism to handle these situations, which may be important for explaining intermediate (1.x) Seyfert galaxies.

Finally, dust emission provides a snapshot of the torus that carries no information about its dynamics. Only molecular line observations can provide information about the kinematics of clouds in the obscuring torus.

Acknowledgments. The support of NSF grant AST-0206149 is gratefully acknowledged. In addition, M.E thanks Chalmers University for a Jubileum Professor award which supported a most enjoyable visit to Onsala Space Observatory.

References

Alonso-Herrero, A., et al. 2001, AJ, 121, 1369

Alonso-Herrero, A., et al. 2003, AJ, 126, 81

Antonucci, R., 1993, ARA&A, 31, 473

Antonucci, R., 2002, in Astrophysical Spectropolarimetry, ed. J. Trujillo-Bueno, F. Moreno-Insertis & F. Sanchez (Cambridge University Press), 151

Bassani L., et al 1999, ApJS, 121, 473

Bock, J.J., et al 2000, AJ, 120, 2904

Efstathiou, A., & Rowan-Robinson, M. 1995, MNRAS, 273, 649

Elvis, M. et al., 1994, ApJS, 95, 1

Granato, G.L. & Danese, L., 1994, MNRAS, 268, 235

Ivezić, Ž., Nenkova, M. & Elitzur, M. 1999, User Manual for DUSTY, Univ. of Kentucky Internal Report[1]

Kartje, J. F., Königl, A., & Elitzur, M, 1999, ApJ, 513, 180

Krabbe, A., Böker, T., & Maiolino, R. 2001, ApJ, 557, 626

Mushotzky, R. F., Cowie, L. L., Barger, A. J., & Arnaud, K. A. 2000, Nature, 404, 459

Natta, A. & Panagia, N., 1984, ApJ, 287, 228

Nenkova, M., Ivezić,Ž. & Elitzur, M. 2002, ApJ Lett., 570, L9 (NIE)

Pier, E., & Krolik, J., 1992, ApJ, 401, 99

Pier, E., & Krolik, J., 1993, ApJ, 418, 673

Risaliti, G., Maiolino, R., & Salvati, M. 1999, ApJ 522, 157

[1]accessible at http://www.pa.uky.edu/∼moshe/dusty/

Risaliti, G., Elvis, M., & Nicastro, F., 2002, ApJ, 571, 234

Rowan-Robinson, M., 1995, MNRAS 272, 737

Sanders, D. et al., 1989, ApJ, 347, 29

Spoon, H.W.W. et al., 2003, A&A, 385, 1022

Wills, B. J. 1999, in ASP Conf. Ser. 162, Quasars and Cosmology, ed. G. Ferland & J. Baldwin (San Francisco: ASP), 101